

Supplementary Material

Two-dimensional GeSe/SnSe heterostructure for high performance thin-film solar cells

Yuliang Mao^{a,*}, Congsheng Xu^a, Jianmei Yuan^b, Hongquan Zhao^c

^a Hunan Key Laboratory for Micro–Nano Energy Materials and Devices, School of Physics and Optoelectronic, Xiangtan University, Hunan 411105, China

^b Hunan Key Laboratory for Computation and Simulation in Science and Engineering, School of Mathematics and Computational Science, Xiangtan University, Hunan 411105, China

^c Chongqing institute of Green and Intelligent Technology, Chinese Academy of Sciences, Chongqing 401120, China

1. Molecular dynamics simulation

To test the thermal stability of the GeSe/SnSe heterostructure, molecular dynamics simulation based on density functional theory (DFT) has been explored [S1-S4]. The simulation is performed within a 4×4 supercell. The time step and total time are set as 1 fs and 10000 fs, respectively. The result indicate that the variation of free energy have slight oscillation with the increasing time, as can be found in Fig. S1. Therefore, the GeSe/SnSe heterostructure can remain stable and robust at room temperature.

*Corresponding author, E-mail: ylmao@xtu.edu.cn

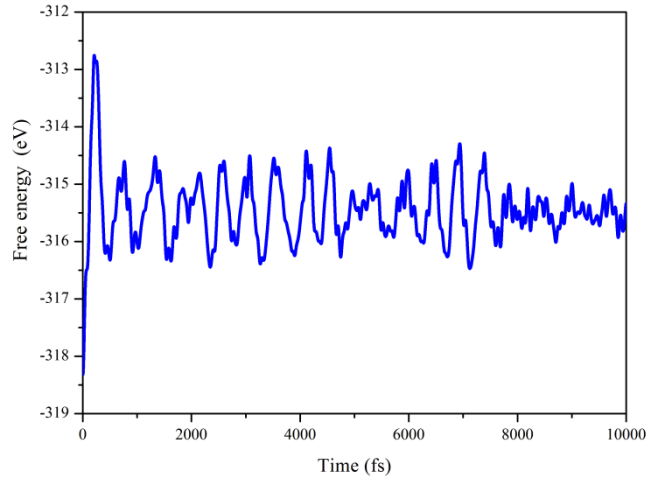


Fig. S1 Evolution curves of the total energies of GeSe/SnSe heterostructure by molecular dynamics simulations at room temperature.

2. The influence of interlayer distance on band gap

The influence of interlayer distance on band gap is very significant for some vertical heterostructure. For example, Tongay et al. [S5] demonstrated experimentally that the band structure of WS₂/MoS₂ vdW heterostructure could be tuned by interlayer distance. Therefore, we calculate the band gap as a function of interlayer distance in GeSe/SnSe heterostructure, which is shown in Fig. S2. It shows that when GeSe/SnSe heterostructure is stretched along the vertical direction from 2.97 Å to 4.57 Å, the band gap is almost linearly decreased from 0.54 eV to 0.44 eV. In contrast, if the GeSe/SnSe heterostructure is compressed to 2.76 Å, the band gap is linearly increased to 0.56 eV. However, the variation value of the band gap is small when applied vertical strain. Therefore, for GeSe/SnSe heterostructure the interlayer distance is negligible factors on the band gap.

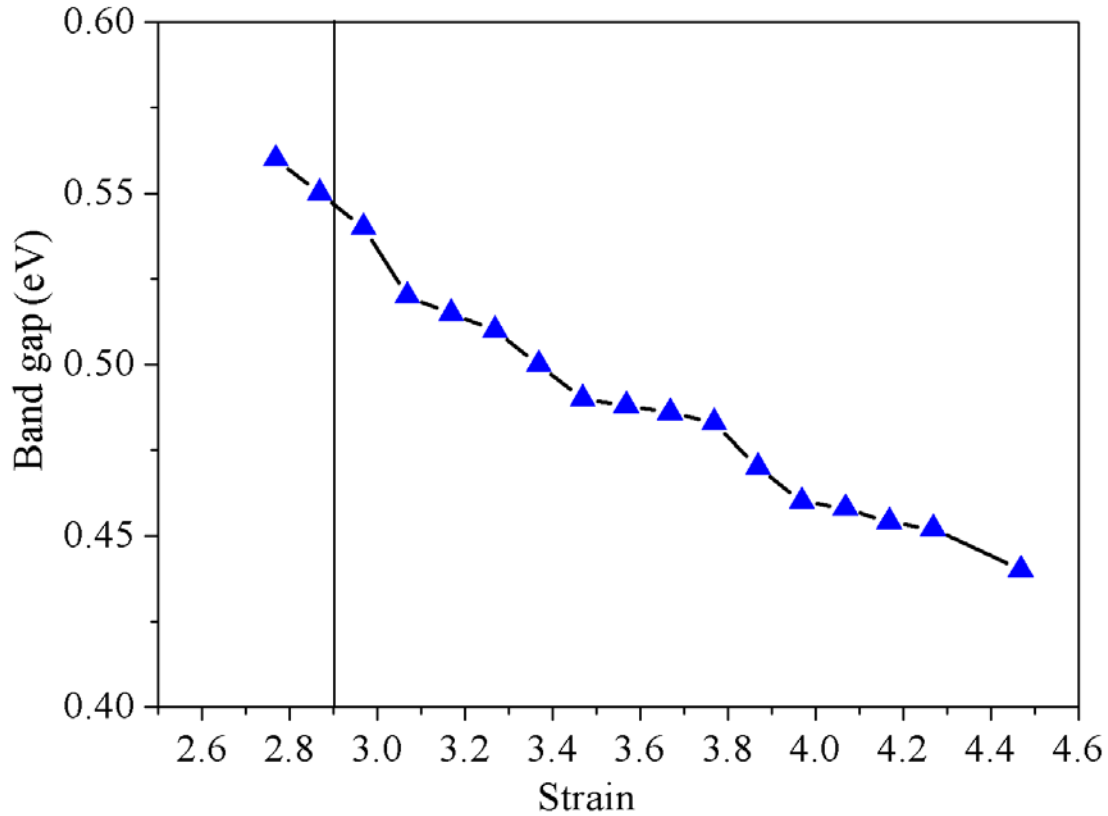


Fig. S2 The variation of band gap under vertical stain for GeSe/SnSe heterostructure

3. The influence of in-plane strain on band gap

The group-IV monochalcogenides have analogy structure as phosphorene. Their pucker structure is very sensitive for in-plane strain [S6-S7]. In Fig. S3, we calculate the influence of in-plane strain on the band gap of GeSe/SnSe heterostructure. As can be found in Fig. S3(a), when applying stretched strain along x direction from 0% to 9%, the variation of band gap is almost linearly increased from 0.54 eV to 1.05 eV. In contrast, if the GeSe/SnSe heterostructure is compressed to -9%, the band gap is linearly decreased to 0 eV, which exhibits a semiconductor to metal transition in energy gap. Moreover, when stretching GeSe/SnSe heterostructure, it keeps inherent feature of direct band gap. However, the transition from direct band gap to indirect band gap has take place under -6% compressed strain. In Fig. S3 (b), when stretched strain is applied along z direction, the variations of

band gap is increased at first and then decreases. In addition, if applying over 6% stretched strain, the direct band gap of GeSe/SnSe heterostructure will be changed to an indirect band gap. As same with that along x direction, the band gap is also decreased under compressed strain. There is also a transition from direct to indirect under the strain of -2%. For bi-axis strain, when stretched strain is applied, the band gap is increasing with the increasing value of strain. However, when compressed strain is applied, the band gap is decreased at first, then it is increased. It finally tends to be reduced. This result shows that the band gap of GeSe/SnSe heterostructure is sensitive under in-plane strain. Moreover, the range of tunable energy gap for GeSe/SnSe is wide, which is in a range of 0 eV to 1.05 eV. Therefore, our result shows that the GeSe/SnSe heterostructure is significantly promising for the applications in optoelectronics.

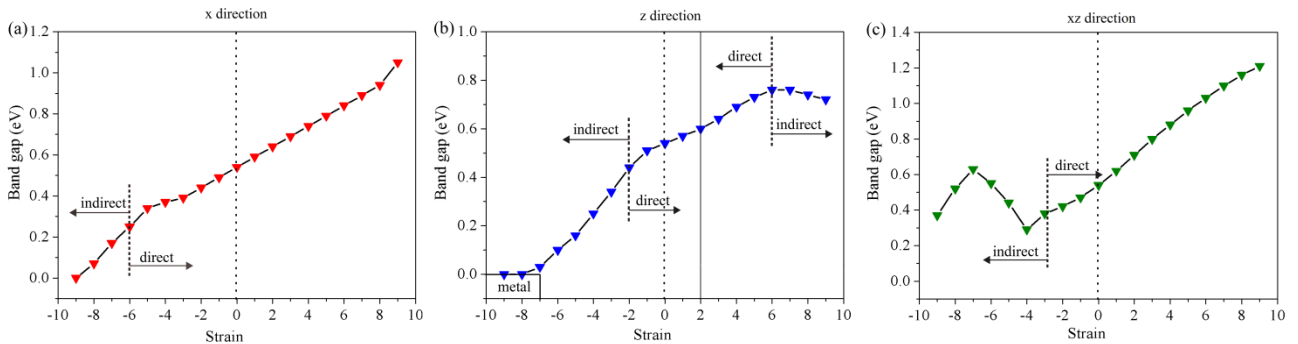


Fig. S3 The variation of band gap under in-plane strains. The value range of σ is from -9% to 9%. The positive and negative value corresponds to stretching and compression strain, respectively. (a)-(c) indicate the results of GeSe/SnSe heterostructure under strains along different directions, (a) σ_x , (b) σ_z , and (c) σ_{xz} , respectively.

4. The comparison of PCE between our results and other reported heterostructures

To further verify our method, we use our method to calculate the PCE and mobility in previous reported materials. For example, we regenerated the PCE of ZrS₃/HfS₃ [S8], InSe/GeSe [S9], phosphorene/MoS₂ [S7], and GeSe/SnS [S10-S11] heterostructures.

TABLE S1. The comparison of PCE between our results and other reported heterostructures. VBO and CBO are the valence band offset and conduction band offset between two monolayer structures, respectively. Donor band gap is refer to the band gap of donor layer. V_{oc} represents the open voltage, while J_{sc} represents the short-circuit current. The denoted PCE is the result obtained from our calculation, while the denoted PCE* are obtained from corresponding published paper for comparison with our calculated result.

Structures	VBO	CBO	Donor bandgap	V_{oc}	J_{sc}	PCE	PCE*
	eV	eV	eV	eV	A	%	%
GeSe/SnSe (Our result)	1.18	0.06	1.48	1.12	0.3	21.47	
GeSe/SnS (Our result)	0.14	0.17	1.59	1.12	0.26	18.79	18
GeSe/SnS [Ref.13-14]	0.29	0.15	1.66	1.21	0.24	18.64	18
ZrS ₃ /HFS ₃ [Ref. 4]	0.08	0.17	1.92	1.45	0.16	15.52	16
Phosphorene/MoS ₂ [Ref. 2]	1.17	0.12	1.03	0.61	0.47	18.48	18

TABLE S2. The calculated effective mass m^* , deformation potential E_l (eV), elastic modulus (Jm^{-2}) and carrier mobility ($10^3 \text{ cm}^2V^{-1}s^{-1}$) of InSe/GeSe heterostructure for electron (e) and hole (h) along x and y direction. The results of InSe/GeSe* are obtained from corresponding paper in the literature [S11] to be compared with our result.

carrier type		Effective mass		deformation potential (eV)		Elastic modulus ($J m^{-2}$)		Mobility ($10^3 \text{ cm}^2 V^{-1} s^{-1}$)	
		(m_0)		E_x	E_y	C_x	C_y	μ_x	μ_y
		m_x	m_y						
	InSe/GeSe	0.316	0.356	5.77	4.72	62.11	101.55	0.41	0.81
electron	InSe/GeSe*	0.208	0.241	6.099	5.331	56.535	95.585	0.7	1.33
hole	InSe/GeSe	0.291	0.361	3.56	8.45	62.11	101.55	1.21	0.26
	InSe/GeSe*	0.189	0.256	4.068	9.310	56.535	95.585	1.75	0.42

Using our method mentioned in our paper, we calculated the PCE of ZrS₃/HFS₃, phosphorene/MoS₂, and GeSe/SnS heterostructures. For GeSe/SnS heterostructure, we calculated its VBO, CBO and donor band gap. For other heterostructures, the VBO, CBO and donor band gap were reported in published works. Our results and previous reported results are listed together to be compared with each other. As shown in Table S1, we can find that there is only minor difference in VBO, CBO and donor band gap of GeSe/SnS [S11-S12] heterostructure between our calculated

results and previous reported values. This minor difference is acceptable due to use different DFT code and different parameters set in SCF calculations. For PCE of GeSe/SnS heterostructure, our predicted result is 18.79%, which is very close to previous reported PCE of 18% [S11]. In addition, for other heterostructures, our predicted PCE is consistent with previous reported values. For example, by our calculations, the PCE of phosphorene/MoS₂ heterostructure is 18.48%. Dai et al. [S7] predicted the PCE of phosphorene/MoS₂ heterostructure is 18%. It can be found that our test result of PCE is consistent with the result reported by Dai et al. We also calculated the mobility of InSe/GeSe heterostructure. Our obtained results are summarized in Table S2 for comparison. As shown in Table S2, our calculated hole mobility of $10^3 \text{ cm}^2\text{V}^{-1}\text{s}^{-1}$ for InSe/GeSe heterostructure has same scale of magnitude as that reported in previous work [S9]. Therefore, we believe that our used method in manuscript is reliable due to the consistent results between our tested cases and the reported values in the literature.

5. Phonon dispersion of monolayer GeSe, monolayer SnSe and GeSe/SnSe heterostructure

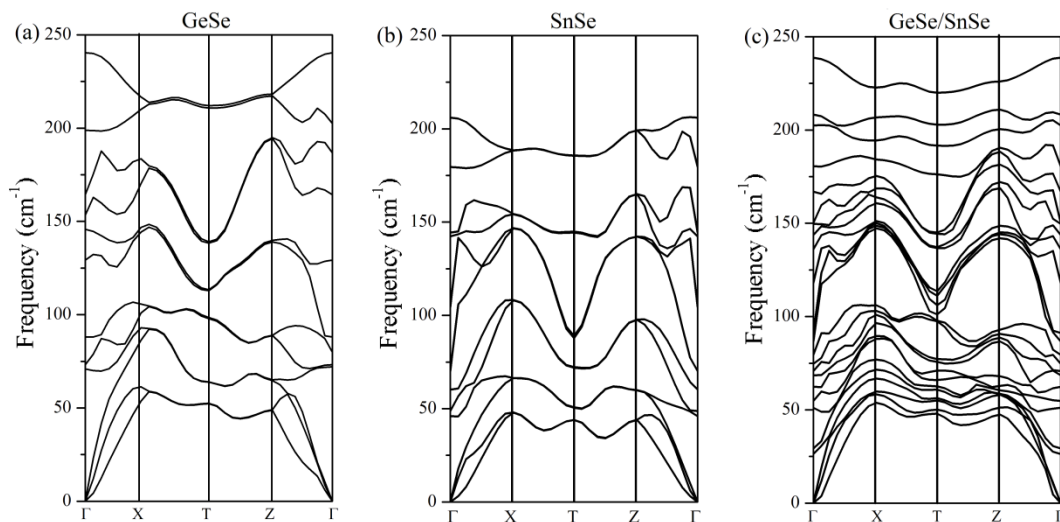


Fig. S4. Phonon spectrum of (a) GeSe, (b) SnSe, and (c) GeSe/SnSe heterostructure

In Fig. S4, we show the calculated phonon dispersion of monolayer GeSe, monolayer SnSe and GeSe/SnSe heterostructure to verify the dynamic stability. Our results indicate that no imaginary frequency is found in the phonon spectrum, which proves that the monolayer GeSe, monolayer SnSe and GeSe/SnSe heterostructure are stable at room temperature.

References

- [S1] Kresse, G., Furthmuller, J. Efficient iterative schemes for ab initio total-energy calculations using a plane-wave basis set. *Phys. Rev. B* **54**, 11169-11186 (1996).
- [S2] Hohenberg, P., Kohn, W. Inhomogeneous electron gas. *Phys. Rev. B* **136**, 864-871 (1964).
- [S3] Blöchl, P. E., Projector augmented-wave method. *Phys. Rev. B* **50**, 17953 (1994).
- [S4] Perdew, J. P., Burke, K., Ernzerhof, M. Generalized gradient approximation made simple. *Phys. Rev. Lett.* **77**, 3865 (1996).
- [S5] Tongay, S.; Fan, W.; Kang, J.; Park, J.; Koldemir, U.; Suh, J.; Narang, D. S.; Liu, K.; Ji, J.; Li, J. B.; Sinclair R.; Wu J. Q., Tuning interlayer coupling in large-area heterostructures with CVD-grown MoS₂ and WS₂ monolayers. 2014, *Nano Letters* **14**(6), 3185.
- [S6] Hu, Y.; Zhang, S.; Sun, S.; Xie, M.; Cai, B.; Zeng, H. J. A. P. L., GeSe monolayer semiconductor with tunable direct band gap and small carrier effective mass. 2015, *Appl. Phys. Lett.* **107** (12), 407-377.
- [S7] Dai, J.; Zeng, X. C., Bilayer phosphorene: Effect of stacking order on bandgap and its potential applications in thin-film solar cells. 2014, *J. Phys. Chem. Lett.* **5** (7), 1289-1293.
- [S8] Zhao Q.; Guo Y.; Y. Zhou et al., Band alignments and heterostructures of monolayer transition metal trichalcogenides MX₃ (M=Zr, Hf; X =S, Se) and dichalcogenides MX₂ (M=Tc, Re; X=S, Se) for solar applications. 2018, *Nanoscale* **10**(7), 3547-3555.
- [S9] Xia C.; Du J.; Huang X. et al., Two-dimensional n-InSe/p-GeSe(SnS) van der Waals heterojunctions: High carrier mobility and broadband performance. 2018, *Phys. Rev. B* **97**(11), 115416.

[S10] X. Lv, W. Wei, C. Mu et al., Two-dimensional GeSe for high performance thin-film solar cell. *J. Phys. Chem. A*, **2018**, *6*(12), 5032-5039.

[S11] Xia C.; Du J.; Xiong W. et al., A type-II GeSe/SnS heterobilayer with suitable direct gap, superior optical absorption and broad spectrum for photovoltaic applications. *J. Phys. Chem. A*, **2017**, *5*(26), 13400-13410.